Classification of ERS-SAR Images for Sea Ice Identification by Texture Analysis with Neural Networks

Lars Kaleschke[1], Axel Bochert[2]

[1]Institute of Environmental Physics, University of Bremen, D-28334 Bremen, Germany; e-mail:lkalesch@thor.physik.uni-bremen.de, phone: +49(0) 421 218 4726, fax: 4555

[2]Alfred-Wegener-Institut für Polar- und Meeresforschung, Columbusstrasse, D-27568 Bremerhaven, Germany; e-mail:abochert@awi-bremerhaven.de

Abstract: This paper investigates the possibility of distinguishing between different sea ice types in Synthetic Aperture Radar (SAR) images recorded with the European Remote Sensing Satellite (ERS-1). The proposed texture classification scheme is evaluated with test images and then used to differ sea ice types in SAR images. Airborne line scanner measurements provide training areas for the texture classifier and serve as ground truth for validation of the classification results. The primary focus of this paper is to study the classification of surface type signatures and not the segmentation of the image. Therefore two error measurements are introduced. First the overall pixel to pixel classification error, and second the pure classification accuracy of large uniform regions. With the presented method it is not possible to distinguish between second- and multi-year ice. But it is possible to distinguish between old ice and medium first-year ice with a pure classification accuracy of about 97%. The overall classification error increases to 20% corresponding to different sea ice coverages.

INTRODUCTION

It is difficult to interprete the Synthetic Aperture Radar (SAR) images recorded with the European Remote Sensing Satellite (ERS-1) since it only operates at one frequency and one polarization for sending and recieving. Additional complications are caused by the multiplicative speckle noise. The ambiguities in the normalized radar cross section (NRCS) do not allow unique assignments to surface types with simple grey-level threshhold techniques. Therefore it is not always possible to distinguish different sea ice types in SAR images using the mean NRCS alone. In many cases the texture is even more meaningful than the mean NRCS [1]. Texture information improves the possibility of distinguishing between different regions with similar NRCS. For each pixel a texture feature vector is calculated considering its surrounding square region. This degrades on the one hand the spatial resolution of the information to be extracted, but on the other hand increases the achievable amount of information. The subsequent classification is done in a multidimensional feature space by the aid of a supervised learning neural network. The proposed texture classification scheme is first evaluated with test images (Brodatz textures) and then with ERS-SAR images of sea ice.

Acknowledgment: AWI contribution 1595.

TEXTURE CLASSIFICATION SCHEME

First texture features have to be extracted from the image. For each pixel a feature vector is calculated using a moving square window including $w \times w$ pixels. The dimension of the feature vector is equal to the number of texture features, in this work eight. The used features are the first order statistical moments: mean, variance to mean ratio, and skewness. In addition to these features derived from the grey level co-occurrence matrix (GLCM): angular second moment, entropy, correlation, inverse difference moment, and contrast (the average of the different directional calculations with a fixed displacement of three pixels) [2]. A traditional method in statistical classification is the development of approximations of the probability density functions, but it is difficult to state the multidimensional probability density function for the investigated cases. Therefore a supervised neural network learning architecture was chosen for classification, namely Kohonen's Learning Vector Quantization (LVQ) [3]. LVQ is based upon the concept of classical Vector Quantization, the approximation of probability density functions by a restricted set of optimally placed discrete parameter vectors. The parameter vectors are called codebook vectors (CV), and the set of CVs is called codebook. The codebook is generated by learning from examples of class labelled feature vectors (training data). Representative examples of all occuring classes have to be selected. The codebook is used for classification of test data. Each CV operates as a minimum distance classifier. The feature vectors derived from the test data are compared to all CVs. The nearest CV wins and its assigned class is the result of classification.

One can expect classification errors in the regions near (dis-

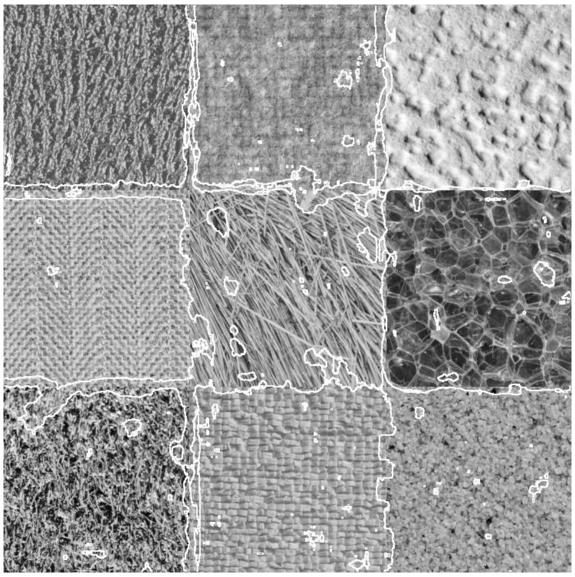

Figure 1: Test image (Brodatz textures). The borderlines derived from the result of classification were overlain in white. The errors are $e_1 = 6.7\%$ (overall) and $e_2 = 1.5\%$ (classification).

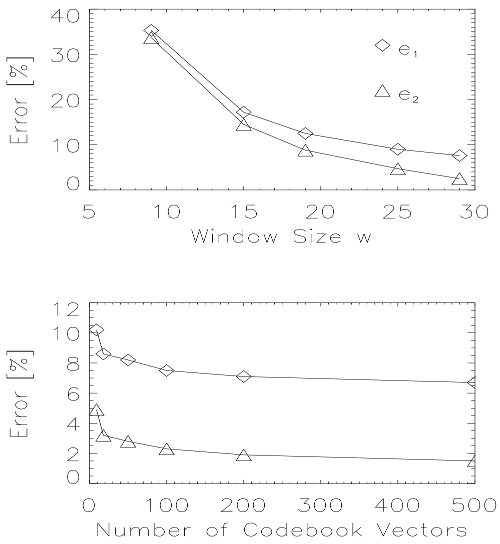

Figure 2: Top:varying window size, 70 CVs. Bottom:varying number of CVs, window size 29×29.

tance $> w/2$) transitions of different textures due to the overlap of the feature extraction window with the size w. This is considered in the estimation of the classification error by defining two error measurements: the overall pixel to pixel error e_1 and the error e_2 without respecting the regions near texture borders. The latter measurement e_2 represents the pure classification error for uniform textured regions rather than the former error e_1 which includes the misclassification due to smearing effects near the borders of different textures. Evaluation of the scheme itself is done with a test image (which serves in this case also as training data) consisting of nine different Brodatz textures (Fig. 1) by varying one system parameter and keeping other parameters constant. The set of test textures have been chosen because they are difficult to classify with simple grey-level threshhold techniques and the classification is not possible with one of the used features alone, with the intention to show the applicatively of the scheme to a broad range of textures. The most important system parameters were found to be the window size w and the number of CVs as shown in Fig. 2. The top of Fig. 2 shows the inherent characteristic; the higher the considerated number of pixels (corresponding to the statistical significance of the classification result) the lower the spatial resolution and vice versa. For the number of CVs equal to the number of classes the classification is a simple minimum distance classification ($e_2 = 5\%$). A larger number of CVs increases the classification accuracy ($e_2 < 2\%$) as shown in the bottom of Fig. 2. The proposed scheme was tested with other images and found to cope with miscellaneous textures and also very noisy data. It is therefore well suited for classification of textured images especially for SAR images.

DATA SET DESCRIPTION

The data used in this study were collected during the aeroplane campaign REFLEX II (Radiation and Eddy Flux Experiment) [4], which took place north of Svalbard (78° N, 15° E) from 28th February to 25th March 1993. The ERS-SAR image (orbit: 8657, frame: 1935) was taken at 12:48 UTC on 12th March 1993. The corresponding area was crossed by the Polar 2 research aircraft (DO228) while recording line scanner images of the sea ice surface from 13:30 to 14:00 UTC. Two different line scanner systems of the Alfred Wegener Institute were mounted on the aeroplane. They are sensitive in the visual and thermal infrared ranges. The data set reflects a winter situation with no open water and very few pixels of young ice types: dark nilas, light nilas, grey ice, grey-white ice, and thin first-year ice. The highest percentage has different types of first-year (medium, and thick), as well as second-year (SY) and multi-year ice (MY).

The line scanner images were corrected for radiometric and geometric distortions, classified by the use of a two-dimensional histogram, and manually matched to ERS-SAR images as described in [1].

CLASSIFICATION OF ERS-SAR IMAGES

The first step of processing the ERS-SAR images is the calibration [5]. In the following we have used images of the square root NRCS, linear scaled on one byte integer (256 grey levels). In contrast to [2] there hasn't be done any equal-probability quantizing before calculating the texture features to assure the

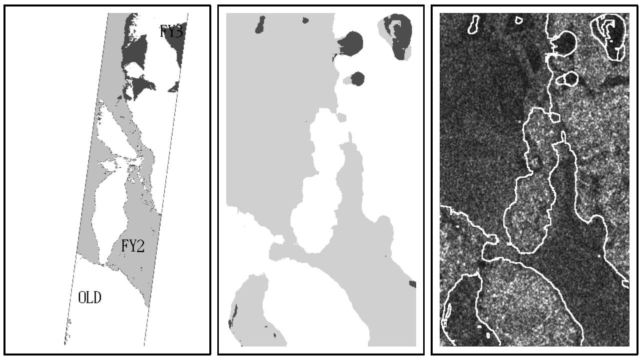

Figure 3: Classified line scanner image (left), classified ERS-SAR image (center), and ERS-SAR image overlain by the edges of the classified ERS-SAR image (right). The images show an area of 6.6 km $\times$ 3.8 km.

Table 1: Classification result corresponding to Fig. 3. The left columns show the overall coverage of ice types and the overall error e_1. The right columns show the coverage of ice types for selected uniform regions (in a distance $d > w/2$ to the borders), in order to determine the pure classification error e_2.

	Overall		Pure	
	Line scan	SAR	Line scan	SAR
	Pixels: 63699		Pixels: 22532	
FY2	33.9 %	33.5 %	22.0 %	21.6 %
FY3	8.2 %	4.0 %	1.5 %	1.4 %
OLD	56.7 %	62.5 %	76.5 %	77.0 %
Others	1.2 %	0.0 %	0.0 %	0.0 %
Errors		e_1=20.4 %		e_2=0.9 %

comparability of different images. The combined SAR and line scanner images were splitted up into 19 partially overlapping clippings (300 $\times$ 530 pixels). The proposed classification scheme was applied on these clippings (window size 29 $\times$ 29, 100 CVs). The clippings served either as training data or as test data. Fig. 3 is an example of the statistically evaluated data set. On the left it shows the classified line scanner image, three ice types are recognised: medium first-year ice (FY2), thick first-year ice (FY3) and old ice (SY and MY). The right image shows the ERS-SAR image overlain by the edges derived from the classification result which is shown in the center of Fig. 3. Table 1 shows the concentrations of the ice types and the classification errors e_1 and e_2 as defined in the previous section. It is obvious, that the overall error $e_1 = 20.4\%$ is larger than the pure classification error $e_2 = 0.9\%$, due to the relatively low resolution of the used feature extraction technique. The primary focus of this investigation is not the precise segmentation but accurate classification (precision in the feature space). From this point of view it is obvious that ice types (e.g. young ice) which cover only a few pixels in the image can not be classified with the proposed method. Young ice falls in the category "others" in table 1. It occurs only in narrow leads. The size of the moving window for feature extraction is larger than the width of the leads in any of the cases in the data set. Therefore this ice type is not detectable with the applied method. The statistical significance is only given for ice types with an occurence on large scales and an adequate percentage in the data set (FY2, SY, and MY). Above conditions disables the evaluation of the complete data set. Six out of the 19 clippings were statistically evaluated, like the clipping in Fig. 3, with the following results. The attempt of distinguishing between SY and MY leads to a large error. Therefore the number of ice types was reduced by integrating this similar ice types into one class of old ice (OLD). The average (over six clippings) overall pixel to pixel classification error is $e_1 = 11\% \pm 7\%$ and the average pure classification error is $e_2 = 1.4\% \pm 1\%$.

CONCLUSIONS

With the above restrictions we can state the following conclusions from the statistical evaluation of the data set. It is not possible to distinguish between ice that survives one summer melt season (second-year ice) and ice that survives more than one summer melt season (multi-year ice) by means of texture in ERS-SAR images. It is possible to distinguish between old ice (second- or multi-year ice) and medium first-year ice. The classification accuracy achieved in this work is more then 97%.

REFERENCES

[1] A. Bochert, "Airborne line scanner measurements for ERS-1 SAR interpretation of sea ice," International Journal of Remote Sensing, 20(2):329–348, 1999.

[2] R.M. Haralick, K. Shanmugam, and L. Dinstein, "Textural features for image classification," IEEE Transactions on Systems Man and Cybernetics, SMC-3(6):610–621, 1973.

[3] T. Kohonen, "Self-Organizing Maps," Springer Series in Information Sciences, 1997.

[4] C. Kottmeier, J. Hartmann, C. Wamser, A. Bochert, C. Lüpkes, D. Freese, and W. Cohrs, "Radiation and eddy flux experiment 1993 (REFLEX II)," Berichte zur Polarforschung 133,Bremerhaven: Alfred-Wegener-Insitut, 1994.

[5] H. Laur, "ERS-1 SAR calibration, derivation of backscatter coefficient σ in ERS-1.SAR.PRI products," European Space Agency, 1992, Technical Note, Issue 1, Rev 0.